

Cite this: *Dalton Trans.*, 2019, **48**, 16322Received 10th September 2019,  
Accepted 27th September 2019

DOI: 10.1039/c9dt03626a

rsc.li/dalton

Nickel(II) PE<sup>1</sup>CE<sup>2</sup>P pincer complexes (E = O, S) for electrocatalytic proton reduction†Sandeep Kaur-Ghumaan,<sup>ID</sup> \*<sup>a,b</sup> Patrick Hasche,<sup>ID</sup> <sup>a</sup> Anke Spannenberg<sup>a</sup> and Torsten Beweries<sup>ID</sup> \*<sup>a</sup>

Nickel(II) chloride and thiolate complexes with <sup>i</sup>PrPE<sup>1</sup>CE<sup>2</sup>P<sup>i</sup>Pr (E = O, S) pincer ligands were investigated as electrocatalysts for the hydrogen evolution reaction in CH<sub>3</sub>CN in the presence of acetic acid and trifluoroacetic acid. The bis(thiophosphinite) (S,S) chloride complex reduced protons at the lowest overpotential in comparison with the bis(phosphinite) (O,O) and mixed phosphinite–thiophosphinite (O,S) complexes. A combination of electrochemical, NMR and UV-vis spectroscopic and mass spectrometric experiments provides mechanistic insights into the catalytic cycle for proton reduction to dihydrogen.

## Introduction

Pincer ligands and their metal complexes have been known since the early 1970s.<sup>1</sup> Since then several new systems with numerous functional groups<sup>2,3</sup> have emerged, and depending on the functional group, have been employed as crystalline switches, as sensors and as precatalysts for a number of stoichiometric and catalytic transformations.<sup>3a</sup> In particular, metal complexes with tridentate pincer ligands have attracted considerable attention in homogeneous catalysis.<sup>4</sup> In this regard, an interesting series of bis(phosphinite) based nickel pincer complexes have been reported by Zargarian *et al.*<sup>5</sup> and Guan *et al.*<sup>6</sup> Based on these reports, very recently, the first Ni thiophosphinite <sup>i</sup>PrPOCSP<sup>i</sup>Pr and Ni bis(thiophosphinite) <sup>i</sup>PrPSCSP<sup>i</sup>Pr (<sup>i</sup>PrPOCSP<sup>i</sup>Pr = C<sub>6</sub>H<sub>4</sub>-1-(SPi-Pr<sub>2</sub>)-3-(OPi-Pr<sub>2</sub>); <sup>i</sup>PrPSCSP<sup>i</sup>Pr = C<sub>6</sub>H<sub>4</sub>-1,3-(SPi-Pr<sub>2</sub>)) pincer complexes were synthesised by our group.<sup>7</sup> The <sup>i</sup>PrPOCSP<sup>i</sup>Pr and <sup>i</sup>PrPSCSP<sup>i</sup>Pr Ni complexes showed significantly better activity than the known isostructural bis(phosphinito) <sup>i</sup>PrPOCOP<sup>i</sup>Pr Ni complex (<sup>i</sup>PrPOCOP<sup>i</sup>Pr = C<sub>6</sub>H<sub>4</sub>-1,3-(OPi-Pr<sub>2</sub>) for Kumada cross-coupling reactions, activating even chlorobenzene at room temperature. In another study, we have shown that Rh bis(thiophosphinite) complexes can be accessed by C–H activation at the PSCSP ligand precursor at room temperature, a behaviour that is

rather unusual as typically such metalation reactions require much higher temperatures.<sup>8</sup>

Because of these findings we were further interested in studying <sup>i</sup>PrPOCSP<sup>i</sup>Pr and <sup>i</sup>PrPSCSP<sup>i</sup>Pr complexes, especially of Ni as a non-noble metal, as catalysts for other reactions, particularly for the electrocatalytic proton reduction to dihydrogen. Though a plethora of complexes with different metals and ligands have been studied for the electrocatalytic and photocatalytic proton reduction to hydrogen in various media,<sup>9</sup> there are only a few Ni pincer complexes that have been investigated and reported as catalysts for the hydrogen evolution reaction (HER) (Fig. 1).<sup>10</sup>

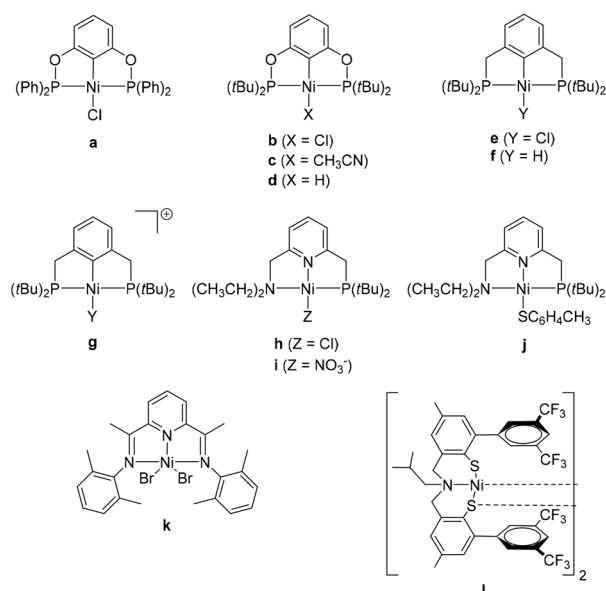


Fig. 1 Ni pincer complexes reported as electrocatalysts for the HER.

<sup>a</sup>Leibniz-Institut für Katalyse e.V. an der Universität Rostock, Albert-Einstein-Str. 29a, 18059 Rostock, Germany. E-mail: skaur@chemistry.du.ac.in, torsten.beweries@catalysis.de

<sup>b</sup>Department of Chemistry, University of Delhi (North Campus), New Delhi-110007, India

† Electronic supplementary information (ESI) available: Electrochemical, UV-vis, NMR, MS, and crystallographic data. CCDC 1893578. For ESI and crystallographic data in CIF or other electronic format see DOI: 10.1039/C9DT03626A

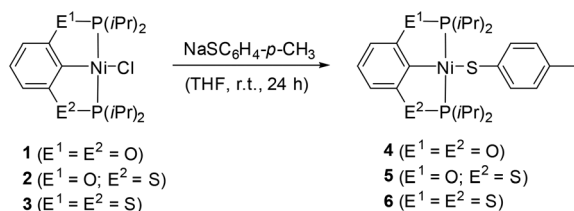
The reported nickel(II) pincer complexes were efficient catalysts (TOF  $\sim 50\text{--}200\text{ s}^{-1}$ ; overpotential  $\sim 0.35\text{--}0.85\text{ V}$ ) for electrocatalytic proton reduction.<sup>10a,d</sup> Moreover, motivated by the recent reports on Ni(II) PCP (**a-g**)<sup>10a,b</sup> and PNN pincer complexes (**h-j**)<sup>11</sup> as electrocatalysts for the HER, we were interested in further studying the influence of different bridging atoms (O,O; O,S; S,S) on the catalytic properties of the complexes. Therefore, four reported  $[(iPr)POCOP(iPr)NiCl]$  **1**,  $[(iPr)POCSP(iPr)NiCl]$  **2**,  $[(iPr)PSCSP(iPr)NiCl]$  **3**,  $[(iPr)POCOP(iPr)NiSC_6H_4CH_3]$  **4** and two new  $[(iPr)POCSP(iPr)NiSC_6H_4CH_3]$  **5** and  $[(iPr)PSCSP(iPr)NiSC_6H_4CH_3]$  **6** complexes were synthesised and investigated for the electrocatalytic reduction of protons to hydrogen in the presence of acetic acid (AA) and trifluoroacetic acid (TFA) in acetonitrile. Based on UV/vis, NMR and MS experiments, a mechanism for the catalytic proton reduction has been proposed.

## Results and discussion

### Synthesis and characterisation of Ni(II) pincer complexes

The Ni(II) chloride complexes  $[(iPr)PE^1CE^2P(iPr)NiCl]$  (E = O,O; O, S; S,S) (**1–3**) were synthesised as reported in the literature.<sup>5,7</sup> The Ni(II) thiolate complex  $[(iPr)POCOP(iPr)NiSC_6H_4CH_3]$  (**4**) was obtained from the reaction of  $[(iPr)POCOP(iPr)NiCl]$  and  $NaSC_6H_4CH_3$ .<sup>6</sup> All analytical data for complex **4** matched well with those reported in the literature.<sup>6</sup> The Ni(II) thiolate complexes  $[(iPr)POCSP(iPr)NiSC_6H_4CH_3]$  (**5**) and  $[(iPr)PSCSP(iPr)NiSC_6H_4CH_3]$  (**6**) were prepared by a procedure similar to that used for complex **4** (Scheme 1).

Crystals of complex **6** suitable for X-ray analysis were obtained from an *n*-hexane solution layered with acetonitrile at  $-30\text{ }^\circ\text{C}$ . The molecular structure of **6** (Fig. 2) shows the Ni(II) centre in a distorted square planar coordination environment with a Ni1–S3 distance of 2.2334(4) Å longer than that observed for the structurally similar bis(phosphinite) complex **4** (2.1908(7) Å).<sup>6</sup> The <sup>1</sup>H NMR spectra of complexes **5** and **6** in THF-*d*<sub>8</sub> displayed the expected peaks for the two isopropyl groups of the pincer ligand, the methyl group of the thiolate ligand and for the aromatic protons present. The <sup>31</sup>P {<sup>1</sup>H} NMR spectrum of complex **5** in THF-*d*<sub>8</sub> displayed two doublets at 107.2 and 180.1 ppm with the value at the lower field corresponding to the P connected to the O atom, while that for complex **6** displayed a singlet at 96.4 ppm.



Scheme 1 Synthesis of Ni(II) thiolate complexes **4–6**.

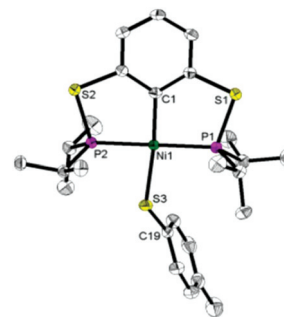


Fig. 2 Molecular structure of complex **6**. Thermal ellipsoids correspond to 30% probability. Hydrogen atoms are omitted for clarity.

### Electrochemical characterisation and proton reduction

The redox properties of the pincer complexes  $[(iPr)PE^1CE^2P(iPr)NiCl]$  (E = O,O; **1**; E = O,S; **2**; and E = S,S; **3**) and  $[(iPr)PE^1CE^2P(iPr)NiSC_6H_4CH_3]$  (E = O,O; **4**; E = O,S; **5**; and E = S,S; **6**) were investigated using electrochemistry in acetonitrile under argon atmosphere. All the potentials are given vs.  $Fc^+/Fc$  (0.1 M *n*-Bu<sub>4</sub>NPF<sub>6</sub>) at 0.1 V s<sup>-1</sup> unless otherwise mentioned. The cyclic voltammograms (CVs) for complexes **1–6** displayed an irreversible one-electron reduction process that can be assigned to a Ni(II)/Ni(I) couple (Table 1 and Fig. S1 and S2†). The reduction potential for the Ni(II)/Ni(I) couple shifted significantly to more positive values on moving from O,O to O,S and S,S bridging atoms in the chloride and thiolate complexes. From the plot of peak current (*i*<sub>p</sub>) of the reduction waves vs. square root of the scan rate (0.025–1 V s<sup>-1</sup>), it can be claimed that the electrochemical processes were diffusion-controlled (Fig. S3†). The complexes also displayed multiple irreversible oxidation processes (Table 1). The complexes were further studied for electrocatalytic proton reduction in the presence of weak and

Table 1 Electrochemical data for complexes **1–6** in acetonitrile

Complex	<i>E</i> <sub>pc</sub> /V	<i>E</i> <sub>pa</sub> /V	<i>E</i> <sub>cat</sub> <sup>a</sup> (η)/V		
			AA	AA with Ag <sup>+</sup>	TFA
<b>1</b>	−2.40	0.51 0.80 1.02	−2.38 (0.92)	−2.03	−1.88 (0.99)
<b>2</b>	−2.25	0.62 0.87 1.06	−2.23 (0.77)	−2.01	−1.73 (0.84)
<b>3</b>	−2.06	0.63 1.05	−2.06 (0.60)	−1.97	−1.65 (0.76)
<b>4</b>	−2.53	0.18 0.89 1.17	−2.52 (1.06)	—	−1.59 (0.70)
<b>5</b>	−2.36	0.23 0.92 1.16	−2.35 (0.89)	—	−1.57 (0.68)
<b>6<sup>b</sup></b>	−2.14	0.30 0.80	—	—	—

<sup>a</sup> Peak current potential value taken for *E*<sub>cat</sub>. <sup>b</sup> No electrocatalytic experiments were done using this complex due to limited solubility in acetonitrile.

strong acids, acetic acid (AA,  $E_{\text{HA}/\text{H}^+}^{\circ} = -1.46$  V,  $\text{p}K_{\text{a}} = 22.3$  in  $\text{CH}_3\text{CN}$ ) and trifluoroacetic acid (TFA,  $E_{\text{HA}/\text{H}^+}^{\circ} = -0.89$  V,  $\text{p}K_{\text{a}} = 12.7$  in  $\text{CH}_3\text{CN}$ ), respectively (Table 1).<sup>12</sup>

In the following section, we describe the electrocatalytic investigations using the above-described complexes. Electrochemical data are shown to be exemplarily for complex 2 only; the corresponding data for all the other complexes are depicted in the ESI.† Upon the addition of a small amount of AA (~2 equiv.), the potential of the reduction peak for each of the complexes remained unchanged. However, increase in current at the complex reduction peaks was recorded in the CVs with a further addition of AA (Fig. 3 and S4–S6†). Since the  $E_{\text{cat}}$  potential was very close to the  $i_{\text{pc}}$  in the absence of acid, it suggests that the reduction of the pre-catalyst with a concomitant release of the chloride or thiolate ligand occurs

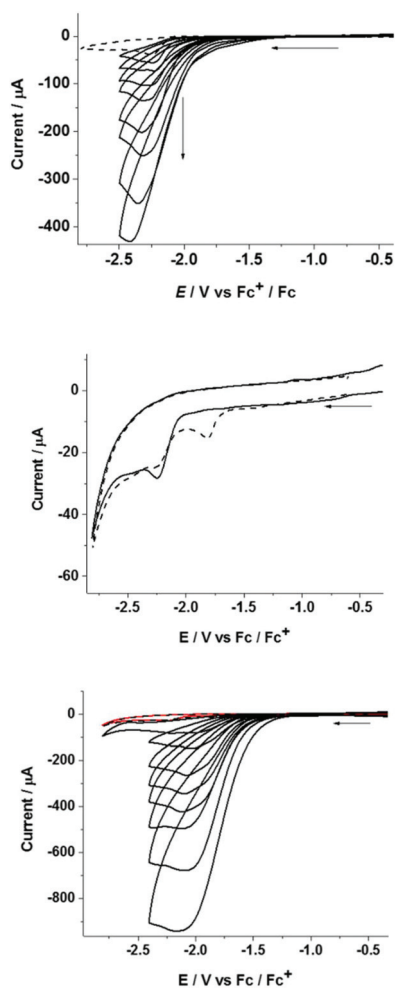


**Fig. 3** Top: CVs for complex 2 (1.47 mM) in MeCN in the absence (---) and presence (—) of (1.55, 3.09, 6.17, 9.24, 15.35, 21.41, 33.41, 45.24 mM) of acetic acid at  $0.1 \text{ V s}^{-1}$ . Centre: CVs for complex 2 (0.44 mM) in MeCN in the absence (—) and presence (---) of  $\text{AgNO}_3$  at  $0.1 \text{ V s}^{-1}$ . Bottom: CVs for complex 2 (0.44 mM) in MeCN in the absence (---) and presence (—) of (0–28 mM) acetic acid with  $0.1 \text{ M TBAP}$  at  $0.1 \text{ V s}^{-1}$ . CVs with acetic acid were measured after the addition of  $\text{AgNO}_3$  to the MeCN solution of the sample.

prior to catalysis. This was further confirmed by CVs measured for the complexes before and after coulometry (one-electron reduction), which showed a significant change in the CV pattern after coulometry (Fig. S7 and S8†). Removal of the chloride ligand was also probed by the addition of  $\text{AgNO}_3$  and gave  $E_{\text{pc}}$  values ( $-1.95$  (for 1),  $-1.82$  (for 2) and  $-1.67$  V (for 3)) close to  $E_{\text{cat}}$  values in the presence of the stronger acid, TFA (Fig. 3, centre). Also, the addition of  $\text{Ag}^+$  during catalysis results in a significant increase in current as well as a shift of the reduction potential (e.g. for 2: from  $-2.23$  V to  $-2.01$  V) (Fig. 3) closer to the value obtained in electrocatalysis with TFA (Table 1, *vide infra*). CVs recorded after bulk electrolysis do not show pronounced waves; however, shoulders can be detected that show the same potential as seen in experiments with  $\text{Ag}^+$  (Fig. 3, S4, S5, S7 and S8†). Next, we added an excess of chloride ions to probe the role of halide elimination. Although we observed a suppression of current, we did not manage to obtain CV patterns that contain valuable information. Based on the above findings it is concluded that reductive removal of the chloride ligand leads to the formation of the solvated complex  $[(^{\text{iPr}}\text{POCSP}^{\text{iPr}})\text{Ni}(\text{MeCN})]^+$  during bulk electrolysis.

When TFA was used as the source of protons instead, the catalytic reduction potential was recorded between  $-1.88$  and  $-1.65$  V for the chloride complexes (1–3) and at  $-1.59$  and  $-1.57$  V for the thiolate complexes 4 and 5, respectively (Fig. S9–S13†). Due to the limited solubility of complex 6 in  $\text{CH}_3\text{CN}$ , electrocatalytic studies were not performed using this species. A similar shift to more positive reduction potentials when increasing the  $\text{p}K_{\text{a}}$  of the proton source was reported earlier by Fan and co-workers.<sup>11a</sup> Notably, these values are in the same range as those found in the experiments with  $\text{Ag}^+$  (*vide supra*), indicating that the formation of the solvated complex  $[(^{\text{iPr}}\text{POCSP}^{\text{iPr}})\text{Ni}(\text{MeCN})]^+$  requires the removal of the chloride ligand either by  $\text{Ag}^+$  or strong acids. Also, curve crossing was observed at low scan rates ( $25 \text{ mV s}^{-1}$  and below), which could be an indication that an ECE mechanism is operative, leading to the formation of a reduced nickel intermediate complex (Fig. S14†).<sup>11</sup>

Without the catalyst, insignificant current was observed between  $-1.0$  to  $-2.6$  V for direct reduction of protons at the glassy carbon working electrode (Fig. S15–S17†).<sup>13</sup> The catalytic behaviour of the complexes (shown for 1 and 4) was further confirmed by bulk electrolysis experiments. The difference in the charge vs. time plots for only acid and for acid with catalyst indicates that the complexes are catalysts for the HER (Fig. S18†). The formation of hydrogen during bulk electrolysis measurements was further confirmed by GC experiments.

The rinse test was performed for the catalysts (1–5) after the bulk electrolysis experiments (Fig. S19 and S20†). No significant peaks were observed in the control experiments and, hence, the catalysis can be assumed to be homogeneous and not because of electrode deposition or complex decomposition. For the control experiments, after electrolysis, the glassy carbon working electrode was removed, rinsed with aceto-

nitrile and dipped into the solution having the same amount of acid but without the catalyst.

The overpotential ( $\eta/V$ ) was calculated using the Evans method (Table 1).<sup>12b</sup> The catalytic efficiencies for the complexes were calculated to be 88 (1), 66 (2), 60 (3), 97 (4) and 77% (5) in AA and 50 (4) and 45% (5) in TFA at low acid concentrations, by using the formula for catalytic efficiency, C.E. =  $(i_{\text{cat}}/i_{\text{p}})/(C_{\text{HA}}/C_{\text{cat}})$  ( $i_{\text{cat}}$  = catalytic current,  $i_{\text{p}}$  = current for reductive peak of the catalyst in the absence of acid,  $C_{\text{HA}}$  = concentration of acid, and  $C_{\text{cat}}$  = concentration of catalyst) as defined by Felton and co-workers.<sup>12b</sup>

The catalytic peak current ( $i_{\text{cat}}$ ) increased linearly with the catalyst concentration [cat], thus indicating that at fixed acid concentrations [acid] the reaction is first-order type with respect to [cat] (Fig. S21 and S22†). The initial linearity of the plots of  $i_{\text{cat}}$  vs. [acid] suggests that catalysis with complexes 1–5 is second-order with respect to acid concentration (Fig. 4 and S23–S25†), which is in line with previous studies on other pincer complexes.<sup>10a</sup> Therefore, the observed rate  $k$  (TOF/s<sup>-1</sup>) is dependent on [acid] under these conditions and can be calculated using eqn (1),<sup>14</sup> where  $n$  is the number of electrons involved in the catalytic reaction (2),  $k$  is the rate constant, and  $\nu$  is the scan rate (0.1 V s<sup>-1</sup>).

$$\frac{i_{\text{cat}}}{i_{\text{p}}} = \frac{n}{0.446} \sqrt{\frac{RTk[\text{acid}]^2}{F\nu}} \quad (1)$$

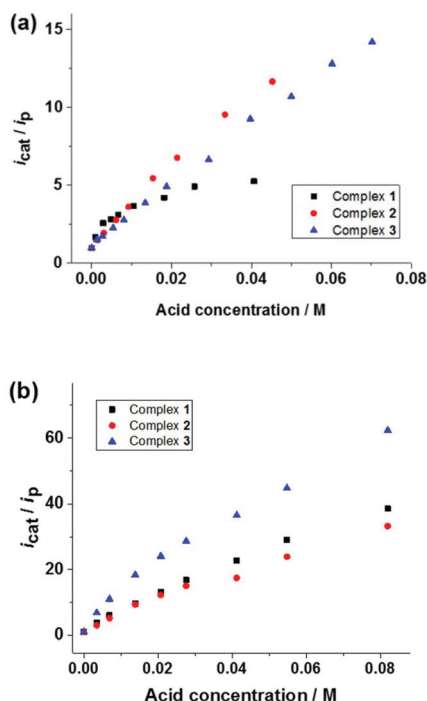


**Fig. 4**  $i_{\text{cat}}/i_{\text{p}}$  vs. acid concentration (M) plots (a) for  $[\text{Pr}^{\text{P}}\text{COP}^{\text{Pr}}]\text{NiCl}$  (1) (1 mM), for  $[\text{Pr}^{\text{P}}\text{CSP}^{\text{Pr}}]\text{NiCl}$  (2) (1.47 mM) and for  $[\text{Pr}^{\text{P}}\text{PSCSP}^{\text{Pr}}]\text{NiCl}$  (3) (1.43 mM) (with acetic acid), and (b) for complexes 1–3 (0.45 mM) with acetic acid after the addition of  $\text{AgNO}_3$  to the MeCN solution of the sample.

For the  $i_{\text{cat}}/i_{\text{p}}$  vs. [acid] and  $k_{\text{obs}}$  vs. amount of acid plots, see Fig. 4 and Fig. S23 and S24.† For plots of  $i_{\text{cat}}$  vs. scan rate see Fig. S26–S32.† The measurements were done with two different AA concentrations for the complexes. Scan rate independence was achieved only at a scan rate of 0.4 V s<sup>-1</sup> or higher (Fig. S26–S30†). The  $k_{\text{obs}}$  (TOF/s<sup>-1</sup>) values for the maximum acid concentration studied were calculated to be 13 (1), 6 (2), 5 (3), 13 (4) and 24 (5) with AA. The TOF values were calculated at the scan rates of 0.4 (1), 0.8 (2), 1.0 (3), 1.0 (4) and 0.8 (5) V s<sup>-1</sup>. No kinetic information could be extracted from the experiments with TFA since a region independent of scan rate was not fully reached even at higher scan rates (Fig. S31 and S32†).

Notably, while for the chloride complexes 1–3, the bis(thiophosphinite) complex 3 showed a higher  $i_{\text{cat}}/i_{\text{p}}$  value, the bis(phosphinite) thiolate complex 4 was superior to its unsymmetrical analogue 5. Taken together with results from previous studies that use thiophosphinite ligands,<sup>7,8,15</sup> this suggests pronounced reactivity differences upon the introduction of sulfur into the backbone of the pincer ligand, the origin of which still requires further studies.

### Mechanistic considerations

In order to get a detailed insight into the mechanism of proton reduction, UV-vis, NMR and mass spectrometric experiments were carried out in the absence and presence of acids. Since the electrocatalytic studies were carried out only for complexes 1–5, titrations with acid were performed only for these five complexes. Unfortunately, with acetic acid, a more resolved set of UV-vis spectra was obtained only for the thiolate complexes that showed clear isosbestic points (Fig. S35†). For titrations with TFA as a stronger acid, small but gradual changes were seen in the UV-vis absorption spectra upon the addition of TFA to the chloride complexes 1–3 and in case of the thiolate complexes 4 and 5 (Fig. 5 and Fig. S33–S35†).

The UV absorption maximum for complex 1 shifted from 335 to 325 nm, and during titration with acid an isosbestic point was preserved at 330 nm. This indicated the formation of a single product complex at all acid concentrations (Fig. 5a). Clear isosbestic points which can be attributed to the formation of monocationic solvent bound species  $[\text{Pr}^{\text{P}}\text{PE}^{\text{Pr}}\text{CE}^{\text{Pr}}\text{P}^{\text{Pr}}]\text{Ni}(\text{MeCN})^+$  of the complexes were observed for all complexes except for bis(thiophosphinite) complex 3. Notably, for complexes 1 and 4, formation of the same new species that possesses the same UV-vis spectroscopic features (*i.e.* isosbestic point at 330 nm and absorption maximum at 325 nm) was observed, suggesting that in both systems the same organometallic species is formed. However, Fig. 5b shows that for 4, formation of this species occurs at much lower acid concentrations, which is in line with the more facile removal of the thiolate ligand upon protonation. A similar behavior was observed for the complex pair 2/5 (Fig. S33 and S35†). The addition of a base such as sodium bicarbonate restored the spectra of the chloride complexes but not the thiolate complexes (Fig. S34 and S35†), which is in line with the fact that for the thiolate complexes protonation of the ligand results in

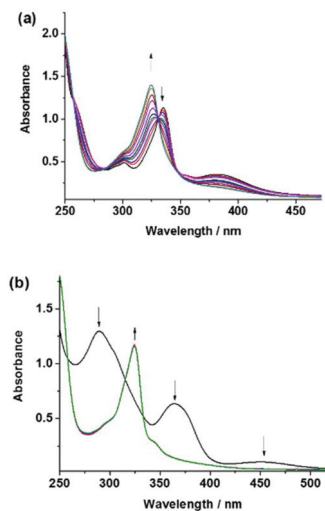
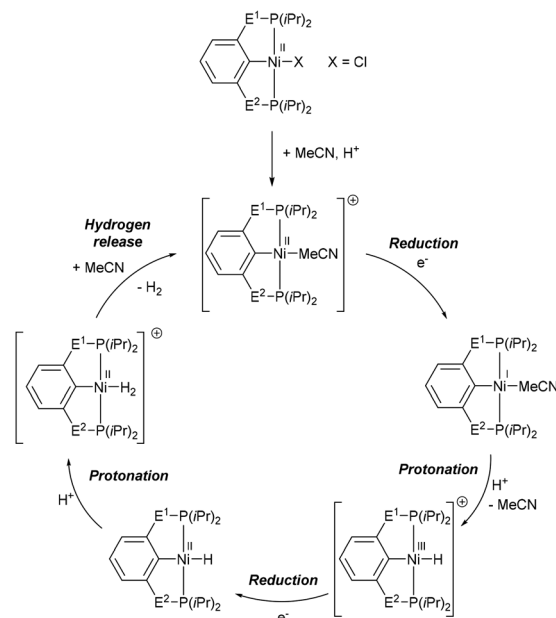


**Fig. 5** UV-vis absorption spectroscopy ( $l = 1$  mm) recorded in acetonitrile for complex (a)  $[(iPr)POCOP(iPr)NiCl]$  (**1**) (0.13 mM) under different concentrations of TFA (0–93 mM) and (b)  $[(iPr)POCOP(iPr)NiSC_6H_4CH_3]$  (**4**) (0.11 mM) under different concentrations of TFA (0–5 mM). The spectral changes upon the addition of increasing amounts of acid are indicated by arrows.



**Scheme 2** Proposed mechanism for proton reduction with chloride complexes **1–3**.

the formation of the thiol, which cannot further coordinate under the reaction conditions.

The  $^1H$  and  $^{31}P$  NMR spectra for the complexes in the absence and presence of TFA also showed shifts in the peaks indicating the formation of a new species upon the addition of acid (Fig. S36–S45<sup>†</sup>). For the thiolate complexes, formation of free thiol  $p\text{-Me-C}_6\text{H}_4\text{-SH}$  can be deduced from a new resonance in the  $^1H$  NMR spectrum at 3.74 ppm. The reactions of complexes with the same pincer ligand (*i.e.* **1/4** and **2/5**) with acid showed formation of the same resonances ( $\delta^{31}P$  for **1/4**: 193.5/192.7,  $\delta^{31}P$  for **2/5**: 190.1, 188.5/190.8, 189.2 ppm), again suggesting that the same Ni pincer complexes form in the presence of acid. The reaction of **3** with TFA is less well-defined, giving more than one species, as evidenced by the  $^1H$  and  $^{31}P$  NMR (Fig. S40 and S41<sup>†</sup>) spectra. LC-MS measurements for complexes **1**, **2** and **4** with TFA confirm the formation of the solvent-bound species  $[(iPr)PE^1CE^2P(iPr)Ni(MeCN)]^+$  (Fig. S46–S48<sup>†</sup>). Notably, this species is only formed in the presence of acid; simple dissolution in MeCN does not furnish this solvent-bound species.

Electrocatalytic proton reduction using Ni pincer complexes was reported earlier and a mechanism has been proposed based on DFT calculations.<sup>10a</sup> Our electrochemical, UV-vis, MS and NMR data on related  $[(iPr)PE^1CE^2P(iPr)NiX]$  systems with the strong acid TFA support the initial acid-mediated removal of the X ligand from the precatalyst to form a solvent-bound intermediate that could in an ECEC (E = electrochemical and C = chemical) mechanistic scenario catalyse proton reduction. Hence, the chloride complexes in this study might be operating through a similar reaction mechanism as described in ref. 10a (Scheme 2). A different mechanism is, however, likely to be operative with AA which is evidenced by the fact that the

$E_{cat}$  values are close to the  $i_{pc}$  values for the complexes in the absence of acid (Table 1). However, the addition of  $Ag^+$  results in the removal of the chloride ligand and the formation of the same species as with the stronger acid TFA. Although the spectroscopic data discussed above are similar for **1/4** and **2/5**, the difference in the catalytic potentials between the complex pairs that possess the same pincer ligand indicates that the chloride and thiolate complexes operate through different processes. The mechanism shown in Scheme 2 should, therefore, only be considered relevant for chloride complexes **1–3**. These mechanistic differences were observed before by Fan and co-workers for complexes Ni pincer chloride, nitrate and thiolate complexes **h–j** (Fig. 1).<sup>11a</sup> The differences in their potentials and thus the reaction mechanisms could be traced back to the differences in the processes involved in the removal of the X ligand.

## Conclusion

In summary, we have presented electrocatalytic proton reduction using a series of well-defined Ni(II) pincer complexes of the type  $[(iPr)PE^1CE^2P(iPr)NiX]$ . Among the chloride complexes **1–3**, with acetic acid as the proton source, complex **3** is the most efficient with the lowest overpotential. Furthermore, the thiolate complexes were found to be more efficient than the chloride complexes. Based on spectroscopic evidence, an ECEC mechanism that agrees with the earlier suggestions for related systems has been proposed for the proton reduction process with chloride complexes in the presence of strong acids. The observed differences indicate that choice of a suitable X ligand and  $PE^1CE^2P$  ligand can lead to more efficient

and robust catalysts. The advantage of PE<sup>1</sup>CE<sup>2</sup>P type ligands is the formation of the terminal hydride species unlike some of the reported {FeFe} models that involve bridging hydride intermediates, which is a limitation to the catalytic conversion of protons to dihydrogen. We are currently looking into the reasons for the observed reactivities and the development of modified, more stable, possibly redox-active thiophosphinite ligands that allow for the reduction of the overpotential of the HER is underway along with the isolation of the hydride intermediates.

## Experimental section

### Materials and methods

All complex syntheses were carried out in an oxygen- and moisture-free argon atmosphere using standard Schlenk and glovebox techniques. THF, acetonitrile and *n*-hexane were dispensed from a solvent purification system (PureSolv, Innovative Technology) and stored under argon. Deuterated solvents were freshly distilled prior to use and were stored over molecular sieves and under argon. Trifluoroacetic acid (TFA) was purchased from Sigma-Aldrich and used without further purification.

<sup>1</sup>H NMR and <sup>31</sup>P{<sup>1</sup>H} NMR spectra were obtained at room temperature using Bruker AV300 or AV400 spectrometers and were referenced internally to the deuterated solvent. All <sup>1</sup>H NMR spectra were referenced using the chemical shifts of residual protio solvent resonances (THF-*d*<sub>8</sub>: δ<sub>H</sub> 1.72, 3.58; CD<sub>3</sub>CN: δ<sub>H</sub> 1.94). Chemical shifts were reported in ppm (δ) relative to tetramethylsilane. For <sup>31</sup>P{<sup>1</sup>H} NMR spectra, 85% H<sub>3</sub>PO<sub>4</sub> was used as an external standard.

Elemental analysis was performed using a Leco TruSpec Micro CHNS analyzer.

Mass spectra (LC-MS) were recorded using an Agilent 1260/6130 Quadrupol LC-MS with electron spray ionisation (ESI), while the high resolution spectra were recorded using a Waters Xevo G2-XS Tof also with electron spray ionisation. Further mass spectra were recorded using a MAT 95XP Thermo Fisher Mass Spectrometer in chemical ionisation (CI) mode.

The UV/vis spectra for the complexes were measured in acetonitrile using a SPECORD S 600 (Analytik Jena) spectrometer.

Electrochemical measurements were conducted in acetonitrile with 0.1 M tetrabutylammonium-hexafluorophosphate (Sigma-Aldrich, electrochemical grade) as the supporting electrolyte that was dried in vacuum at 383 K. Cyclic voltammetry was carried out using an Autolab potentiostat (PGSTAT204). The working electrode for cyclic voltammetry was a glassy carbon disc (diameter 3 mm, freshly polished). For bulk electrolysis experiments, a carbon rod was used. Platinum was used as the counter electrode. The reference electrode was a non-aqueous Ag/Ag<sup>+</sup> electrode (CH Instruments, 0.01 M AgNO<sub>3</sub> in acetonitrile). All the potentials are quoted against the ferrocene-ferrocenium couple (Fc<sup>+</sup>/Fc); ferrocene was added as an

internal standard at the end of the experiments. For the electrochemical measurements all solutions were prepared using dry acetonitrile (Sigma-Aldrich, spectroscopic grade, dried with molecular sieves 3 Å).

The generation of hydrogen in the bulk electrolysis experiment was determined by gas chromatography. A GC sample was taken from the reaction system and was analysed by the system-GC, Agilent Technologies 6890N/Carboxen 1000/TCD/Methaniser/FID. Gas integration was calibrated using certified gas mixtures from commercial suppliers (Linde and Air Liquide) with the following gas vol%: H<sub>2</sub>: 2500 ppm and 5000 ppm; 1% and 5%. The system allowed for the determination of H<sub>2</sub> within the range, H<sub>2</sub> ≥ 0.25–100 vol%.

### General procedure for NMR and LC-MS experiments

In a glovebox, a J. Young NMR tube was charged with 0.025 mmol of the complex, which was dissolved in 0.5 mL of CD<sub>3</sub>CN before trifluoroacetic acid was added (0.25 mmol). The NMR tube was sealed with a cap and <sup>1</sup>H, <sup>19</sup>F and <sup>31</sup>P NMR spectra were recorded. The next day, the NMR tube was introduced to the glovebox again. Inside the glovebox, the NMR solution was completely transferred to a GC vial and 1 mL of acetonitrile was added to dilute the sample for LC-MS. The vial was closed with a cap and transferred to a small Schlenk flask. The Schlenk flask was eventually opened right before the sample was measured.

### Synthetic procedures

All three Ni-chlorido-complexes, [<sup>i</sup>PrPOCOP<sup>i</sup>Pr]NiCl (1),<sup>5</sup> [<sup>i</sup>PrPOCSP<sup>i</sup>Pr]NiCl (2)<sup>7</sup> and [<sup>i</sup>PrPSCSP<sup>i</sup>Pr]NiCl (3)<sup>7</sup> were prepared as described in the literature.

**Synthesis of [<sup>i</sup>PrPOCOP<sup>i</sup>Pr]NiSC<sub>6</sub>H<sub>4</sub>CH<sub>3</sub> (4).** A solution of [<sup>i</sup>PrPOCOP<sup>i</sup>Pr]NiCl (105 mg, 0.24 mmol) in 15 mL of THF was added to NaSC<sub>6</sub>H<sub>4</sub>CH<sub>3</sub> (142 mg, 0.97 mmol) in a Schlenk flask. An immediate color change from yellow to orange could be observed. The resulting orange suspension was stirred for 24 h at room temperature followed by filtration to afford a clear orange solution. All volatiles were then removed under vacuum and the residue was extracted with 10 mL of acetonitrile. Again, all volatiles were removed under vacuum and the residue was extracted with *n*-hexane (2 × 10 mL). Removal of the solvent under vacuum afforded the product in excellent purity as a solid yellow compound. All analytical data matched with those reported in the literature.<sup>6</sup> <sup>1</sup>H NMR (THF-*d*<sub>8</sub>, 300 MHz, δ): 1.19–1.38 (m, PCH(CH<sub>3</sub>)<sub>2</sub>, 24H), 2.10 (sept, <sup>3</sup>J<sub>H-H</sub> = 7.0 Hz, PCH(CH<sub>3</sub>)<sub>2</sub>, 4H), 2.20 (s, CH<sub>3</sub>, 3H), 6.37 (d, <sup>3</sup>J<sub>H-H</sub> = 8.0 Hz, ArH, 2H), 6.81 (d, <sup>3</sup>J<sub>H-H</sub> = 8.0 Hz, ArH, 2H), 6.87 (t, <sup>3</sup>J<sub>H-H</sub> = 7.9 Hz, ArH, 1H), 7.28 (d, <sup>3</sup>J<sub>H-H</sub> = 8.0 Hz, ArH, 2H). <sup>31</sup>P{<sup>1</sup>H} NMR (THF-*d*<sub>8</sub>, 121 MHz, δ): 188.25 (s).

**[<sup>i</sup>PrPOCSP<sup>i</sup>Pr]NiSC<sub>6</sub>H<sub>4</sub>CH<sub>3</sub> (5).** [<sup>i</sup>PrPOCSP<sup>i</sup>Pr]NiSC<sub>6</sub>H<sub>4</sub>CH<sub>3</sub> (5) was prepared in 58% yield by a procedure similar to that used for 4. <sup>1</sup>H NMR (THF-*d*<sub>8</sub>, 300 MHz, δ): 1.19–1.52 (m, PCH(CH<sub>3</sub>)<sub>2</sub>, 24H), 1.96–2.11 (m, S-PCH(CH<sub>3</sub>)<sub>2</sub>, 2H), 2.20 (s, CH<sub>3</sub>, 3H), 2.31–2.45 (m, O-PCH(CH<sub>3</sub>)<sub>2</sub>, 2H), 6.38–6.46 (m, Ni-ArH<sub>S-meta</sub>, 1H), 6.76–6.86 (m, ArH, 4H), 7.30 (d, <sup>3</sup>J<sub>H-H</sub> = 8.0 Hz, S-ArH<sub>ortho</sub>, 2H). <sup>13</sup>C{<sup>1</sup>H} NMR (THF-*d*<sub>8</sub>, 100 MHz, δ): 16.9 (s, PCH(CH<sub>3</sub>)<sub>2</sub>),

18.3 (s, PCH(CH<sub>3</sub>)<sub>2</sub>), 18.4 (d,  $J_{C-P} = 5.2$  Hz, PCH(CH<sub>3</sub>)<sub>2</sub>), 19.3 (d,  $J_{C-P} = 5.2$  Hz, PCH(CH<sub>3</sub>)<sub>2</sub>), 20.8 (s, CH<sub>3</sub>), 28.3 (d,  $J_{C-P} = 16.0$  Hz, PCH(CH<sub>3</sub>)<sub>2</sub>), 29.1 (d,  $J_{C-P} = 21.5$  Hz, PCH(CH<sub>3</sub>)<sub>2</sub>), 107.8 (d,  $J_{C-P} = 13.4$  Hz, Ni-ArC<sub>S-meta</sub>), 116.8 (d,  $J_{C-P} = 12.4$  Hz, Ni-ArC<sub>O-meta</sub>), 128.0 (s, Ni-ArC<sub>para</sub>), 128.7 (s, S-ArC<sub>meta</sub>), 132.9 (s, S-ArC<sub>para</sub>), 134.9 (s, S-ArC<sub>ortho</sub>), 142.7 (s, S-ArC<sub>ipso</sub>), 149.1 (s, Ni-ArC<sub>S-ortho</sub>), 155.5 (s, Ni-ArC<sub>O-ortho</sub>), 167.5 (s, Ni-ArC<sub>ipso</sub>). <sup>31</sup>P{<sup>1</sup>H} NMR (THF-*d*<sub>8</sub>, 121 MHz,  $\delta$ ): 107.2 (d,  $^2J_{P-P} = 314$  Hz), 180.1 (d,  $^2J_{P-P} = 314$  Hz). Anal. Calcd for C<sub>25</sub>H<sub>38</sub>NiOP<sub>2</sub>S<sub>2</sub>: C, 55.67; H, 7.10; S, 11.89. Found: C, 55.90; H, 7.120; S, 12.68. MS (CI positive, isobutane):  $m/z = 538$  [M]<sup>+</sup>, 415 [M - SC<sub>6</sub>H<sub>4</sub>-*p*-CH<sub>3</sub>].

[<sup>iPr</sup>PSCSP<sup>iPr</sup>]NiSC<sub>6</sub>H<sub>4</sub>CH<sub>3</sub> (6). [<sup>iPr</sup>PSCSP<sup>iPr</sup>]NiSC<sub>6</sub>H<sub>4</sub>CH<sub>3</sub> (6) was prepared in 59% yield by a procedure similar to that used for 4. Crystallisation from an *n*-hexane solution layered with acetonitrile at -30 °C yielded crystals suitable for X-ray analysis. <sup>1</sup>H NMR (THF-*d*<sub>8</sub>, 300 MHz,  $\delta$ ): 1.25–1.52 (m, PCH(CH<sub>3</sub>)<sub>2</sub>, 24H), 2.20 (s, CH<sub>3</sub>, 3H), 2.29–2.44 (sept,  $^3J_{H-H} = 7.0$  Hz, PCH(CH<sub>3</sub>)<sub>2</sub>, 4H), 6.69 (t,  $^3J_{H-H} = 7.6$  Hz, Ni-ArH<sub>para</sub>, 1H), 6.84 (d,  $^3J_{H-H} = 7.6$  Hz, S-ArH<sub>meta</sub>, 2H), 6.88 (d,  $^3J_{H-H} = 7.6$  Hz, Ni-ArH<sub>meta</sub>, 2H), 7.34 (d,  $^3J_{H-H} = 7.6$  Hz, S-ArH<sub>ortho</sub>, 2H). <sup>13</sup>C{<sup>1</sup>H} NMR (THF-*d*<sub>8</sub>, 100 MHz,  $\delta$ ): 18.3 (s, PCH(CH<sub>3</sub>)<sub>2</sub>), 19.7 (s, PCH(CH<sub>3</sub>)<sub>2</sub>), 20.7 (s, CH<sub>3</sub>), 28.5 (t,  $J_{C-P} = 9.7$  Hz, PCH(CH<sub>3</sub>)<sub>2</sub>), 119.2 (t,  $J_{C-P} = 6.0$  Hz, Ni-ArC<sub>meta</sub>), 126.5 (s, Ni-ArC<sub>para</sub>), 128.9 (s, S-ArC<sub>meta</sub>), 132.8 (s, S-ArC<sub>para</sub>), 134.4 (s, S-ArC<sub>ortho</sub>), 141.3 (s, S-ArC<sub>ipso</sub>), 155.5 (s, Ni-ArC<sub>ortho</sub>), 164.7 (s, Ni-ArC<sub>ipso</sub>). <sup>31</sup>P{<sup>1</sup>H} NMR (THF-*d*<sub>8</sub>, 121 MHz,  $\delta$ ): 96.38 (s). Anal. Calcd For C<sub>25</sub>H<sub>38</sub>NiP<sub>2</sub>S<sub>3</sub>: C, 54.06; H, 6.90; S, 17.32. Found: C, 54.04; H, 7.20; S, 17.56 (determined by at least two measurements). MS (CI positive, isobutane):  $m/z = 554$  [M]<sup>+</sup>, 431 [M - SC<sub>6</sub>H<sub>4</sub>-*p*-CH<sub>3</sub>].

### Crystallographic details

X-ray analysis was performed using a Bruker Kappa APEX II Duo diffractometer with Mo-K $\alpha$  radiation. The structure was solved by direct methods (SHELXS-97)<sup>16</sup> and refined by full-matrix least square procedures on  $F^2$  (SHELXL-2014).<sup>17</sup> Diamond was used for graphical representations.<sup>18</sup> CCDC 1893578 contains the supplementary crystallographic data for this paper.†

### Conflicts of interest

There are no conflicts to declare.

### Acknowledgements

We thank our technical and analytical staff, in particular Benjamin Andres. Financial support by the DFG (grant no. BE 4370/5-1) is gratefully acknowledged.

### Notes and references

1 C. J. Moulton and B. L. Shaw, *J. Chem. Soc., Dalton Trans.*, 1976, 1020–1024.

- 2 (a) K. Umehara, S. Kuwata and T. Ikariya, *Inorg. Chim. Acta*, 2014, **413**, 136–142; (b) M. U. Raja, R. Ramesh and K. H. Ahn, *Tetrahedron Lett.*, 2009, **50**, 7014–7017; (c) R. A. Begum, D. Powell and K. Bowman-James, *Inorg. Chem.*, 2006, **45**, 964–966; (d) T. A. Betley, B. A. Qian and J. C. Peters, *Inorg. Chem.*, 2008, **47**, 11570–11582; (e) M. Bröring, C. Kleeberg and E. Cónsul Tejero, *Eur. J. Inorg. Chem.*, 2007, **2007**, 3208–3216; (f) H. A. Burkill, N. Robertson, R. Vilar, A. J. P. White and D. J. Williams, *Inorg. Chem.*, 2005, **44**, 3337–3346; (g) J. A. Camerano, A.-S. Rodrigues, F. Rominger, H. Wadehohl and L. H. Gade, *J. Organomet. Chem.*, 2011, **696**, 1425–1431; (h) S.-A. Filimon, D. Petrovic, J. Volbeda, T. Bannenberg, P. G. Jones, C.-G. Freiherr von Richthofen, T. Glaser and M. Tamm, *Eur. J. Inorg. Chem.*, 2014, **2014**, 5997–6012; (i) T.-A. Koizumi, T. Teratani, K. Okamoto, T. Yamamoto, Y. Shimoi and T. Kanbara, *Inorg. Chim. Acta*, 2010, **363**, 2474–2480; (j) B. K. Langlotz, H. Wadehohl and L. H. Gade, *Angew. Chem., Int. Ed.*, 2008, **47**, 4670–4674; (k) D. C. Sauer and H. Wadehohl, *Polyhedron*, 2014, **81**, 180–187; (l) L. Wang, H.-R. Pan, Q. Yang, H.-Y. Fu, H. Chen and R.-X. Li, *Inorg. Chem. Commun.*, 2011, **14**, 1422–1427; (m) Q. Q. Wang, R. A. Begum, V. W. Day and K. Bowman-James, *Inorg. Chem.*, 2012, **51**, 760–762; (n) Q. Q. Wang, R. A. Begum, V. W. Day and K. Bowman-James, *J. Am. Chem. Soc.*, 2013, **135**, 17193–17199.
- 3 Selected overviews: (a) M. Albrecht and G. van Koten, *Angew. Chem., Int. Ed.*, 2001, **40**, 3750–3781, (*Angew. Chem.*, 2001, **113**, 3866–3898); (b) M. E. van der Boom and D. Milstein, *Chem. Rev.*, 2003, **103**, 1759–1792; (c) M. A. W. Lawrence, Y. A. Jackson, W. H. Mulder, P. M. Bjoremark and M. Hakansson, *Aust. J. Chem.*, 2015, **68**, 731–741; (d) *The Chemistry of Pincer Compounds*, ed. D. Morales-Morales and C. Jensen, Elsevier, Amsterdam, 2007; (e) D. Morales-Morales, *Mini-Rev. Org. Chem.*, 2008, **5**, 141–152; (f) M. E. O'Reilly and A. S. Veige, *Chem. Soc. Rev.*, 2014, **43**, 6325–6369; (g) S. Chakraborty, P. Bhattacharya, H. Dai and H. Guan, *Acc. Chem. Res.*, 2015, **48**, 1995–2003; (h) M. Asay and D. Morales-Morales, in *The Privileged Pincer-Metal Platform: Coordination Chemistry & Applications*, ed. G. van Koten and R. A. Gossage, Springer International Publishing, Cham, 2016, p. 239.
- 4 (a) J. I. van der Vlugt and J. N. H. Reek, *Angew. Chem., Int. Ed.*, 2009, **48**, 8832–8846, (*Angew. Chem.*, 2009, **121**, 8990–9004); (b) J. Choi, A. H. R. MacArthur, M. Brookhart and A. S. Goldman, *Chem. Rev.*, 2011, **111**, 1761–1779; (c) M. Albrecht and M. M. Lindner, *Dalton Trans.*, 2011, **40**, 8733–8744; (d) G. van Koten and D. Milstein, *Organometallic Pincer Chemistry*, Springer, Berlin, 2013, vol. 40; (e) K. J. Szabo and O. F. Wendt, *Pincer and Pincer-Type Complexes: Applications in Organic Synthesis and Catalysis*, Wiley-VCH, Weinheim, 2014.
- 5 (a) V. Pandarus and D. Zargarian, *Organometallics*, 2007, **26**, 4321–4334; (b) B. Vabre, F. Lindeperg and D. Zargarian, *Green Chem.*, 2013, **15**, 3188–3194.

- 6 J. Zhang, A. Adhikary, K. M. King, J. A. Krause and H. Guan, *Dalton Trans.*, 2012, **41**, 7959–7968.
- 7 P. Hasche, M. Joksche, G. Vlachopoulou, H. Agarwala, A. Spannenberg and T. Beweries, *Eur. J. Inorg. Chem.*, 2018, **2018**, 676–680.
- 8 G. Vlachopoulou, S. Möller, J. Haak, P. Hasche, H. J. Drexler, D. Heller and T. Beweries, *Chem. Commun.*, 2018, **54**, 6292–6295.
- 9 (a) U. J. Kilgore, J. A. S. Roberts, D. H. Pool, A. M. Appel, M. P. Stewart, M. R. DuBois, W. G. Dougherty, W. S. Kassel, R. M. Bullock and D. L. DuBois, *J. Am. Chem. Soc.*, 2011, **133**, 5861–5872; (b) M. C. Smith, J. E. Barclay, S. P. Cramer, S. C. Davies, W.-W. Gu, D. L. Hughes, S. Longhurst and D. J. Evans, *J. Chem. Soc., Dalton Trans.*, 2002, 2641–2647; (c) B. J. Fisher and R. Eisenberg, *J. Am. Chem. Soc.*, 1980, **102**, 7361–7363; (d) P. A. Jacques, V. Artero, J. Pecaut and M. Fontecave, *Proc. Natl. Acad. Sci. U. S. A.*, 2009, **106**, 20627–20632; (e) C. Baffert, V. Artero and M. Fontecave, *Inorg. Chem.*, 2007, **46**, 1817–1824; (f) J. P. Bigi, T. E. Hanna, W. H. Harman, A. Chang and C. J. Chang, *Chem. Commun.*, 2010, **46**, 958–960; (g) J. L. Dempsey, B. S. Brunschwig, J. R. Winkler and H. B. Gray, *Acc. Chem. Res.*, 2009, **42**, 1995–2004; (h) R. M. Kellett and T. G. Spiro, *Inorg. Chem.*, 1985, **24**, 2373–2377; (i) J. C. Manton, C. Long, J. G. Vos and M. T. Pryce, *Dalton Trans.*, 2014, **43**, 3576–3583; (j) W. R. McNamara, Z. Han, C.-J. Yin, W. W. Brennessel, P. L. Hollan and R. Eisenberg, *Proc. Natl. Acad. Sci. U. S. A.*, 2012, **109**, 15594–15599; (k) C. Tard, X. Liu, S. K. Ibrahim, M. Bruschi, L. D. Gioia, S. C. Davies, X. Yang, L.-S. Wang, G. Sawers and C. J. Pickett, *Nature*, 2005, **433**, 610–613; (l) W. Gao, J. Ekstrom, J. Liu, C. Chen, L. Eriksson, L. Weng, B. Akermark and L. Sun, *Inorg. Chem.*, 2007, **46**, 1981–1991; (m) P. Surawatanawong, J. W. Tye, M. Y. Darensbourg and M. B. Hall, *Dalton Trans.*, 2010, **39**, 3093–3104; (n) W. T. Eckenhoff and R. Eisenberg, *Dalton Trans.*, 2012, **41**, 13004–13021; (o) M. Kobayashi, S. Masaoka and K. Sakai, *Angew. Chem., Int. Ed.*, 2012, **51**, 7431–7434.
- 10 (a) O. R. Luca, J. D. Blakemore, S. J. Konezny, J. M. Praetorius, T. J. Schmeier, G. B. Hunsinger, V. S. Batista, G. W. Brudvig, N. Hazari and R. H. Crabtree, *Inorg. Chem.*, 2012, **51**, 8704–8709; (b) S. Ramakrishnan, S. Chakraborty, W. W. Brennessel, C. E. D. Chidsey and W. D. Jones, *Chem. Sci.*, 2016, **7**, 117–127; (c) O. R. Luca, S. J. Konezny, J. D. Blakemore, D. M. Colosi, S. Saha, G. W. Brudvig, V. S. Batista and R. H. Crabtree, *New J. Chem.*, 2012, **36**, 1149–1152; (d) A. Mondragon, M. Flores-Alamo, P. R. Martinez-Alanis, G. Aullon, V. M. Ugalde-Saldivar and I. Castillo, *Inorg. Chem.*, 2015, **54**, 619–627.
- 11 (a) C. P. Yap, Y. Y. Chong, T. S. Chwee and W. Y. Fan, *Dalton Trans.*, 2018, **47**, 8483–8488; (b) Y. X. C. Goh, H. M. Tang, W. L. J. Loke and W. Y. Fan, *Inorg. Chem.*, 2019, **58**, 12178–12183.
- 12 (a) G. A. N. Felton, R. S. Glass, D. L. Lichtenberger and D. H. Evans, *Inorg. Chem.*, 2006, **45**, 9181–9184; (b) G. A. N. Felton, C. A. Mebi, B. J. Petro, A. K. Vannucci, D. H. Evans, R. S. Glass and D. L. Lichtenberger, *J. Organomet. Chem.*, 2009, **694**, 2681–2699; (c) L. C. Song, L. Zhu, F. Q. Hu and Y. X. Wang, *Inorg. Chem.*, 2017, **56**, 15216–15230; (d) V. Fourmond, P. A. Jacques, M. Fontecave and V. Artero, *Inorg. Chem.*, 2010, **49**, 10338–10347; (e) A. D. Nguyen, M. D. Rail, M. Shanmugam, J. C. Fettinger and L. A. Berben, *Inorg. Chem.*, 2013, **52**, 12847–12854.
- 13 B. D. McCarthy, D. J. Martin, E. S. Rountree, A. C. Ullman and J. L. Dempsey, *Inorg. Chem.*, 2014, **53**, 8350–8361.
- 14 M. L. Helm, M. P. Stewart, R. M. Bullock, M. R. DuBois and D. L. DuBois, *Science*, 2011, **333**, 863–866.
- 15 (a) J. M. Serrano-Becerra, S. Hernández-Ortega and D. Morales-Morales, *Inorg. Chim. Acta*, 2010, **363**, 1306–1310; (b) W. Yao, X. Jia, X. Leng, A. S. Goldman, M. Brookhart and Z. Huang, *Polyhedron*, 2016, **116**, 12–19; (c) W. Yao, Y. Zhang, X. Jia and Z. Huang, *Angew. Chem., Int. Ed.*, 2014, **53**, 1390–1394.
- 16 G. Sheldrick, *Acta Crystallogr., Sect. A: Found. Crystallogr.*, 2008, **64**, 112–122.
- 17 G. Sheldrick, *Acta Crystallogr., Sect. C: Struct. Chem.*, 2015, **71**, 3–8.
- 18 Diamond - Crystal and Molecular Structure Visualization, Crystal Impact - Dr. H. Putz & Dr. K. Brandenburg GbR, Kreuzherrenstr. 102, 53227 Bonn, Germany, <http://www.crystalimpact.com/diamond>.